R. & M. No. 3011
(17,782)
A.R.C. Technical Report

MINISTRY OF SUPPLY

AERONAUTICAL RESEARCH COUNCIL
REPORTS AND MEMORANDA

The Aerodynamic Effects of Aspect Ratio and Sweepback on Wing Flutter

By

W. G. Molyneux, B.Sc., and H. Hall, B.Sc.

LONDON: HER MAJESTY'S STATIONERY OFFICE

1957

PRICE 5*s* 6*d* NET

The Aerodynamic Effects of Aspect Ratio and Sweepback on Wing Flutter

By

W. G. Molyneux, B.Sc., and H. Hall, B.Sc.

Communicated by the Principal Director of Scientific Research (Air), Ministry of Supply

Reports and Memoranda No. 3011*

February, 1955

Summary.—The report describes tests to obtain direct measurements of the aerodynamic effects of aspect ratio and sweepback on wing flutter. The tests were made on rigid wings with root flexibilities.

It is shown that measured effects of aspect ratio and sweepback on the flutter of these wings can be represented quite closely in flutter calculations based on two-dimensional flow theory by multiplying the two-dimensional aerodynamic coefficients by appropriate factors. The effect of sweepback is represented by multiplying all aerodynamic coefficients by cos Λ, where Λ is the wing leading-edge sweepback, and the effect of aspect ratio is represented by multiplying the aerodynamic damping coefficients by $1/f(A)$ and the stiffness coefficients by $1/[f(A)]^2$ where A is the aspect ratio.

For the wings tested an average value for $f(A)$ is $f(A) = \{1 + (0{\cdot}8/A)\}$.

1. *Introduction.*—Typical aircraft wings that differ in aspect ratio or sweepback normally differ also in other properties that influence the flutter characteristics. It is desirable, however, to have a good general indication of the influence on flutter of the aerodynamic effects of aspect ratio and sweepback alone.

In an earlier report[1] a method was described for segregating the aerodynamic effects of aspect ratio on the flutter of unswept wings by flutter testing wings that are virtually rigid in themselves but are flexibly supported at the root. In the present report the method is extended to determine the aerodynamic effects of both sweepback and aspect ratio on wing flutter. The method is applied to unswept, swept, tapered and inverse tapered wings.

It is shown that a close estimate of the flutter speeds and frequencies of these wings can be obtained on the basis of two-dimensional aerodynamic theory using simple factors for aspect ratio and sweepback effects. These factors apply strictly to the rigid-wing modes employed and to the low speeds used in the tests, but they may be of assistance in flutter prediction for actual aircraft wings.

2. *Basis of the Investigation.*—2.1. *The Basic Principle.*—The flutter equations of motion written in matrix form are :

$$\left[-(a+\gamma)\omega^2 + ib\frac{V}{c_m}\omega + c\frac{V^2}{c_m^2} + e\right]q = 0\,, \qquad \ldots \quad \ldots \quad \ldots \quad (1)$$

* R.A.E. Report Structures 175, received 3rd August, 1955.

where a, e = matrices of structural inertia and elastic coefficients

γ, b, c = matrices of aerodynamic inertia, damping and stiffness coefficients

ω = flutter frequency

V = flutter speed

c_m = wing mean chord

q = column matrix of generalised co-ordinates.

Now suppose that equations (1) refer to a set of finite aspect-ratio, untapered, unswept wings that have the same non-dimensional values of structural and aerodynamic coefficients when the aerodynamic coefficients are computed using two-dimensional theory. With this condition satisfied it has been shown[1] that, with a constant mean chord, the aerodynamic effects of aspect ratio on flutter in roll and pitch freedoms alone may be represented by a relationship of the form:

$$V = V_0 f(A) , \quad .. \quad .. \quad .. \quad .. \quad .. \quad .. \quad (2)$$

where V = flutter speed of the finite aspect-ratio wing

V_0 = calculated flutter speed based on two-dimensional (infinite aspect-ratio) aerodynamic derivatives

A = aspect ratio.

A relationship of this form is obtained from equations (1) if we multiply the aerodynamic damping coefficients in the equations by $1/f(A)$ and the aerodynamic stiffness coefficients by $1/[f(A)]^2$. On this basis the flutter equations for the finite aspect-ratio wing may be written:

$$\left[- (a + \gamma)\omega^2 + i \frac{b}{f(A)} \frac{V}{c_m} \omega + \frac{c}{[f(A)]^2} \frac{V^2}{c_m^2} + e \right] q = 0 \quad .. \quad .. \quad (3)$$

where, as $A \to \infty$, $f(A) \to 1$ and $V \to V_0$. Now consider the infinite aspect-ratio untapered swept wing, and suppose that with the aerodynamic effects of sweep omitted, the infinite swept wing has the same non-dimensional values for structural and aerodynamic coefficients as the infinite unswept wing. It has been shown by Jordan[2] that the aerodynamic effects of sweepback are then represented in the flutter equations by multiplying the aerodynamic coefficients for the unswept wing by the cosine of the angle of sweepback. Therefore for the infinite swept wing the flutter equations are:

$$\left[- (a + \gamma \cos \Lambda)\omega^2 + ib \cos \Lambda \frac{V}{c_m} \omega + c \cos \Lambda \frac{V^2}{c_m^2} + e \right] q = 0 , \quad .. \quad .. \quad (4)$$

where Λ = angle of sweepback.

If there are no secondary effects of aspect ratio on the sweepback factor, we may then suppose that the equations for the finite aspect-ratio swept wing may be written:

$$\left[- (a + \gamma \cos \Lambda)\omega^2 + \frac{ib \cos \Lambda}{f(A)} \frac{V}{c_m} \omega + \frac{c \cos \Lambda}{[f(A)]^2} \frac{V^2}{c_m^2} + e \right] q = 0 . \quad .. \quad .. \quad (5)$$

To include possible secondary effects of aspect ratio on the sweepback factor, the equations may finally be generalised to:

$$\left[- \{a + \gamma F(\Lambda, A)\} \omega^2 + ib \frac{F(\Lambda, A)}{f(A)} \frac{V}{c_m} \omega + c \frac{F(\Lambda, A)}{f(A)^2} \frac{V^2}{c_m^2} + e \right] q = 0 , \quad .. \quad .. \quad (6)$$

where $F(\Lambda, A) \to \cos \Lambda$ as $A \to \infty$

$\to 1 \qquad \Lambda \to 0 .$

It is assumed in equations (6) that the function $F(\Lambda,A)$ can be applied equally to all the aerodynamic coefficients, and it will be seen later (section 6) that this assumption is justified. The main purpose of the present tests was to obtain values for the functions $F(\Lambda,A)$ and $f(A)$ to enable a reasonable estimate of the flutter characteristics of finite aspect-ratio swept wings to be obtained on the basis of two-dimensional theory.

2.2. *Flutter Coefficients for Rigid Wings with Roll and Pitch Freedoms.*—Tests were made on six sets of wings with the plan-forms shown in Fig. 1. Only two of the wings in each set are shown, indicating the upper and lower limits of the particular parameters being varied. The wings were virtually rigid (*i.e.*, were of very high stiffness as compared with the root stiffnesses) and had root flexibilities in roll about an axis at the root parallel to the air-stream, and in pitch about an axis at a constant fraction of the chord aft of the wing leading edge. The flutter coefficients for wings with these two degrees of freedom may be written as follows:

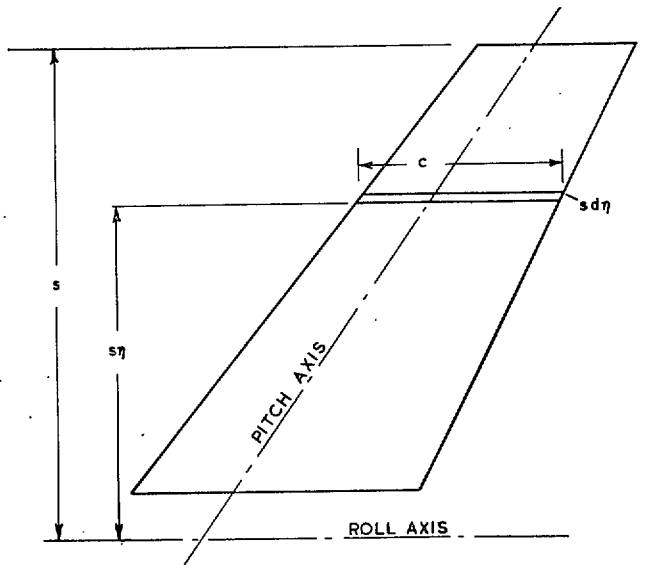

$f = \eta$ = bending (roll) mode of pitch axis with unit value at wing tip

$F = 1$ = twisting (pitch) mode of streamwise wing strips about axes in the wing plane that are normal to the strip and pass through the point of intersection of the strip with the pitch axis.

Aerodynamic coefficients

Inertia	Damping	Stiffness
$\gamma_{11} = \int \left(\frac{c}{c_m}\right)^2 f^2 l_{\ddot{z}}\, d\eta$	$b_{11} = \int \frac{c}{c_m} f^2 l_{\dot{z}}\, d\eta$	$c_{11} = \int f^2 l_z\, d\eta$
$\gamma_{12} = \int \left(\frac{c}{c_m}\right)^3 f F l_{\ddot{\alpha}}\, d\eta$	$b_{12} = \int \left(\frac{c}{c_m}\right)^2 f F l_{\dot{\alpha}}\, d\eta$	$c_{12} = \int \frac{c}{c_m} f F l_{\alpha}\, d\eta$
$\gamma_{21} = -\int \left(\frac{c}{c_m}\right)^3 f F m_{\ddot{z}}\, d\eta$	$b_{21} = -\int \left(\frac{c}{c_m}\right)^2 f F m_{\dot{z}}\, d\eta$	$c_{21} = -\int \frac{c}{c_m} f F m_z\, d\eta$
$\gamma_{22} = -\int \left(\frac{c}{c_m}\right)^4 F^2 m_{\ddot{\alpha}}\, d\eta$	$b_{22} = -\int \left(\frac{c}{c_m}\right)^3 F^2 m_{\dot{\alpha}}\, d\eta$	$c_{22} = -\int \left(\frac{c}{c_m}\right)^2 F^2 m_{\alpha}\, d\eta$

(7)

$l_{\ddot{z}}$, $l_{\ddot{\alpha}}$, $m_{\ddot{z}}$, $m_{\ddot{\alpha}}$, *etc.*, are the two-dimensional aerodynamic strip derivatives referred to the pitch axis.

Structural coefficients

Inertia	Stiffness
$a_{11} = \frac{1}{\rho c_m^2} \int f^2 m\, d\eta$	$e_{11} = a_{11}\omega_{11}^2$
$a_{12} = a_{21} = \frac{1}{\rho c_m^3} \int f F m \bar{x}\, d\eta$	$e_{12} = e_{21} = 0$
$a_{22} = \frac{1}{\rho c_m^4} \int F^2 m K^2\, d\eta$	$e_{22} = a_{22}\omega_{22}^2$

(8)

where

$m\, d\eta$ is the mass of a streamwise wing strip

$m\bar{x}\,d\eta$ is the mass moment of a streamwise wing strip about an axis in the plane of the wing that is normal to the strip and passes through the point of intersection of the strip with the pitch axis

$mK^2\,d\eta$ is the mass moment of inertia of a streamwise strip about an axis in the plane of the wing that is normal to the strip and passes through the point of intersection of the strip with the pitch axis.

Now suppose that we evaluate the aerodynamic coefficients for the six sets of wings of Fig. 1, using equations (7) based on two-dimensional derivatives and with sweepback effects on the derivatives ignored. It is apparent that for each set of wings corresponding aerodynamic coefficients are equal.

Further, wings 1a, 1b, 1c, 1e and 1f are designed to be of solid homogeneous construction and the mass, mass moment and mass moment of inertia per unit span at a wing section $s\eta$ from the root is the same for all the wings in a particular set. Therefore, by equations (8), corresponding inertia coefficients for each set of wings are equal, and corresponding stiffness coefficients are equal if the frequencies of corresponding modes are equal.

The set of wings 1d are also solid and homogeneous in construction but the section normal to the leading edge, rather than the streamwise section, is maintained constant for all the wings. Corresponding inertia coefficients are therefore proportional to the cosine of the angle of sweepback and, with the frequencies of corresponding modes equal, corresponding stiffness coefficients vary in the same way.

The wings shown in Fig. 1a were used to investigate aspect-ratio effects on flutter with sweep effects absent, wings 1b to investigate aspect-ratio effects on flutter for wings of constant sweep angle, wings 1c to investigate sweepback effects on flutter for wings of constant aspect ratio, and wings 1d were used to investigate the effects on flutter of simultaneous variations of aspect ratio and sweepback. The sweepback and aspect-ratio functions obtained from these tests were then applied in the flutter calculations for wings 1e and 1f to obtain an indication of the extent to which the results for untapered wings could be applied to tapered wings.

3. *Details of the Wings.*—All wings were of solid, homogeneous construction with a balsa-wood nose forward of the 30 per cent chord line and spruce aft of this line. The wing section used throughout was RAE 101.

3.1. *Variable Aspect Ratio—Unswept Wings* (*Fig.* 1a).—Tests on this plan-form have already been reported[1] but it was thought advisable to repeat the work because of changes in the test rig.

The main structural details of the wings are given in Table 1. There were eight wings in all covering the range of aspect ratio from 6 to 2; the thickness/chord ratio of the wing section was 0·1.

3.2. *Variable Aspect Ratio—Constant Sweepback Wings* (*Fig.* 1b).—The main structural details are given in Table 2. There were eight wings in all covering the range of aspect ratio from 6 to 2. The construction was similar to that of the unswept wings. However, to obtain aspect ratios corresponding to those of the unswept wings an increased length of wing (as measured along the sweep axis) was required; and to maintain the stiffness of the wings it was necessary to increase the thickness/chord ratio of the streamwise section to 0·15.

3.3. *Constant Aspect Ratio—Variable Sweep Wings* (*Fig.* 1c).—The main structural details are given in Table 3. There were six wings in all covering the range of sweepback from 0 deg to 60 deg. The streamwise chord was constant for all the wings and the thickness/chord ratio of streamwise sections was 0·1.

3.4. *Variable Aspect Ratio—Variable Sweep Wings* (*Fig.* 1d).—The main structural details are given in Table 4. There were five wings in all covering the range of aspect ratio from 2·67 to 1·72 and the range of sweepback from 0 deg to 50 deg. The wing length from roll axis to wing

tip, measured normal to the roll axis, was constant and a constant wing section normal to the wing leading edge was maintained. The thickness/chord ratio of this section was 0·1. The streamwise chord, therefore, varied as the secant of the angle of sweepback and the thickness/chord ratio of streamwise sections varied as the cosine of the angle of sweepback.

3.5. *Variable Aspect Ratio—Tapered and Inverse Tapered Wings* (*Figs.* 1e *and* 1f).—The main structural details are given in Tables 5 and 6. There were eight wings in each set covering the range of aspect ratio from 6 to 2. The thickness of the wings was maintained constant along the span, and this enabled the tapered wings to be inverted to provide inverse tapered wings without modifying the attachment of the wings to the flutter rig. However, the thickness/chord ratio varied over the wing span and ranged from 0·15 for the minimum chord to 0·075 for the maximum. It may be noted that the sweep angles of the leading and trailing edges of the wings vary with aspect ratio.

4. *Description of the Flutter Test Rig.*—The lay-out of the rig is shown diagrammatically in Fig. 2. The roll axis is 0·075 span from the wing root, and the pitch axis is 0·35 chord aft of the wing leading edge and can be rotated to accord with the wing sweepback. Torsion bars of adjustable length on the roll and pitch axes provide variable roll and pitch stiffness, and sliding weights enable adjustment of roll inertia. The rig pitch inertia is negligible compared with the minimum wing pitch inertia and the roll pitch product of inertia of the rig is zero; means of varying these inertias are, therefore, not required. Ball bearings are used on the roll and pitch axes and the friction damping present is small.

5. *Test Procedure.*—The flutter tests were made in the Royal Aircraft Establishment 5-ft Diameter Open Jet Wind Tunnel. The wings were mounted vertically with a reflector plate at the root end to simulate the symmetric airflow conditions. A pitot traverse above the reflector plate showed the flow to be reasonably uniform at the wing position (Fig. 3).

5.1. *Adjustment of Structural Coefficients.*—With the wing in position the roll inertia weight was adjusted so that the required value of roll inertia (wings and mounting) was obtained. The uncoupled frequencies of the rig in roll and pitch were measured by disturbing the rig in one freedom, with the other locked, and counting the cycles of the decaying oscillation by an electrical recorder over a time interval of about fifty cycles of oscillation. The fact that such a large number of cycles could be counted indicates the low structural damping present in the rig. The torsion bars were adjusted so that the frequencies of corresponding modes were the same for all wings of a particular set.

5.2. *Flutter Tests.*—The tunnel speed was increased, the wing being disturbed continually, until a speed was reached at which flutter occurred. The flutter frequency was then measured and the tunnel speed at which the flutter oscillations just died away was taken as the flutter speed.

6. *Comparison of Measured and Calculated Results.*—The results for the variable aspect-ratio unswept and constant sweep wings (Figs. 1a and 1b) are shown in Fig. 4. For both sets of wings the flutter speed varies approximately as $\{1 + (0{\cdot}8/A)\}$*, increasing as the aspect ratio decreases, *i.e.*, for these wings the function $f(A)$ of equations (6) is:

$$f(A) = \left(1 + \frac{0{\cdot}8}{A}\right) \quad \ldots \quad \ldots \quad \ldots \quad \ldots \quad \ldots \quad (9)$$

With this value for $f(A)$ applied to the two-dimensional aerodynamic coefficients the calculated values for flutter speed and frequency of the unswept wings are in very close agreement with those measured.

---

* This compares with the result obtained in earlier tests[1].

$$f(A) = \left(1 + \frac{0.78}{A}\right)$$

For the constant sweep wings the above value for $f(A)$ was used and it was assumed that :

$$F(\Lambda,A) = \cos \Lambda \; . \qquad .. \qquad .. \qquad .. \qquad .. \qquad .. \qquad (10)$$

With these values applied to the two-dimensional coefficients, as in equations (6), the calculated flutter speeds are in very close agreement with those measured, but the agreement of flutter frequencies is not as close. However, to a first approximation, it would appear that the secondary effects of aspect ratio on the sweepback factors can be neglected; and furthermore the sweep factor appropriate to two-dimensional flow, *i.e.*, cos Λ, is applicable at this particular sweepback.

The results for the constant aspect-ratio, variable sweep wings (Fig. 1c) are shown in Fig. 5. Calculations were made using $f(A) = \{1 + (0{\cdot}8/A)\}$ and $F(\Lambda,A) = \cos \Lambda$ as aspect-ratio and sweepback factors applied to the two-dimensional coefficients, and the calculated values of both flutter speed and frequency are in close agreement with those measured.

The above values of $f(A)$ and $F(\Lambda,A)$ thus appear to be satisfactory for calculations on rigid, untapered, swept wings of finite aspect ratio. It may be that the poor agreement obtained between the measured and calculated flutter frequencies of the constant sweepback wings may be due to some effect of thickness/chord ratio on flutter. It will be remembered (section 3) that these wings were given a thickness/chord ratio of $0{\cdot}15$, whereas for the wings of Figs. 1a and 1c the ratio was $0{\cdot}10$.

The results of the tests on the variable aspect-ratio, variable sweepback wings (Fig. 1d) confirm the above factors. If we presume that $f(A) = \{1 + (0{\cdot}8/A)\}$ and $F(\Lambda,A) = \cos \Lambda$, then it is readily shown from equations (6), (7) and (8) (see also section $2{\cdot}1$) that for these wings, for which c_m is proportional to sec Λ, the flutter speeds will vary as $\{1 + (0{\cdot}8/A)\}$ sec Λ. It can be seen from Fig. 6 that the results calculated using the above factors are in quite good agreement with those measured.

The above values of $f(A)$ and $F(\Lambda,A)$ have also been used in the calculations for the tapered and inverse tapered wings (Figs. 1e and 1f), with Λ referring to the sweepback of the wing leading edge. The comparison with the measured results is shown in Fig. 7. A quite close agreement of measured and calculated results is obtained for the tapered wings, but the order of agreement is not as good for the inverse tapered wings. It would appear that a more powerful aspect-ratio factor is required for the latter, but even for this somewhat unusual plan-form the calculated flutter speeds are within 7 per cent of the measured values.

7. *The Glauert Aspect Ratio Function.*—It is of interest to note that the values of the function $1/\{1 + (0{\cdot}8/A)\}^2$ are in quite close agreement with those of the functions $A/(2 + A)$ for a very wide range of aspect ratio. The latter function is that obtained by Glauert[3] as a correction to the slope of the lift curve in two-dimensional steady flow for finite aspect-ratio unswept wings with an elliptic load distribution. Glauert's result is based on theory and is not strictly applicable to rectangular wings; its agreement with the measured result for oscillating wings is, therefore, probably nothing more than coincidence. However, it may be that a measurement in steady flow of the variation of the slope of the lift curve (or some related parameter, *e.g.*, rolling moment) between the wings of a given set would provide an adequate indication of the values of $\cos \Lambda/[f(A)]^2$, and hence $f(A)$, to be used in the flutter equations. It is worth noting that values of this function could be obtained in steady flow for a rigid wing distorted in a mode corresponding to that used in flutter calculations on a flexible wing. A direct measurement of sweepback and aspect-ratio effects on the flutter of flexible wings is not possible by the method used here for rigid wings, as the required adjustment of the flutter coefficients is too complex.

8. *Conclusions.*—The measured aerodynamic effects of aspect ratio and sweepback on wing flutter speeds and frequencies can be represented quite closely in flutter calculations based on two-dimensional flow theory by multiplying the two-dimensional aerodynamic coefficients by

appropriate factors. The effects of sweepback are represented by multiplying the aerodynamic coefficients by cos Λ, where Λ is the sweepback of the wing leading edge, and the aspect-ratio effects are represented by multiplying the aerodynamic damping coefficients by $1/f(A)$ and the stiffness coefficients by $1/[f(A)]^2$, where A is the aspect ratio. The function $f(A)$ is affected by wing taper ratio but a value $f(A) = \{1 + (0{\cdot}8/A)\}$ gives calculated speeds that are within plus or minus 7 per cent of those measured for the wings tested here.

These results apply strictly to rigid wings with root flexibilities fluttering at low speeds, but they may be of assistance in flutter prediction for flexible swept wings of finite aspect ratio.

Acknowledgement.—The authors wish to acknowledge the assistance given by Mr. E. W. G. Chapple in the design of the rig and in the conduct of the tests.

REFERENCES

No.	*Author*	*Title, etc.*
1	W. G. Molyneux and E. W. Chapple ..	The aerodynamic effects of aspect ratio on flutter of unswept wings. R. & M. 2942. November, 1952.
2	P. F. Jordan	General consideration of the flutter of swept wings. R.A.E. Report Struct. 61. A.R.C. 13,307. February, 1950.
3	H. Glauert	*The elements of aerofoil and airscrew theory.* Chapter XI, para. 11.31. Cambridge University Press.

TABLE 1

Variable Aspect Ratio—Unswept Wings

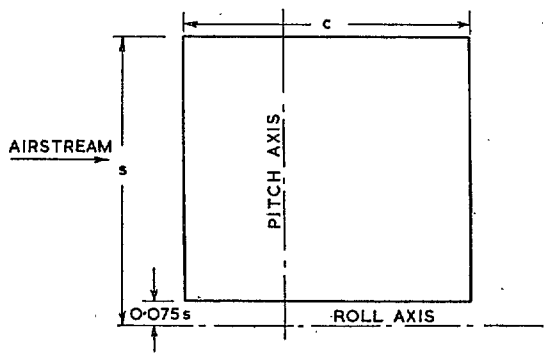

Wing chord, c = 0·5 ft

$\frac{\text{Wing thickness}}{\text{Wing chord}}$ = 0·10

Wing section = RAE 101

$\frac{\text{Distance of pitch axis aft of leading edge}}{\text{Wing chord}}$ = 0·35

Wing length root to tip s (in.)	Wing aspect ratio ($A = 2s/c$)	Inertias—wing plus mounting (slugs ft²)		
		Roll inertia	Roll–pitch cross inertia	Pitch inertia
6	2·00	$1·20 \times 10^{-3}$	$1·02 \times 10^{-4}$	$10·8 \times 10^{-5}$
7	2·33	$1·94 \times 10^{-3}$	$1·40 \times 10^{-4}$	$12·5 \times 10^{-5}$
8	2·67	$2·85 \times 10^{-3}$	$1·67 \times 10^{-4}$	$13·1 \times 10^{-5}$
9	3·00	$3·93 \times 10^{-3}$	$2·02 \times 10^{-4}$	$13·6 \times 10^{-5}$
10	3·33	$5·38 \times 10^{-3}$	$2·50 \times 10^{-4}$	$15·2 \times 10^{-5}$
12	4·00	$9·62 \times 10^{-3}$	$3·21 \times 10^{-4}$	$18·4 \times 10^{-5}$
15	5·00	$18·55 \times 10^{-3}$	$5·17 \times 10^{-4}$	$22·9 \times 10^{-5}$
18	6·00	$31·50 \times 10^{-3}$	$7·60 \times 10^{-4}$	$26·9 \times 10^{-5}$

Uncoupled wing roll frequency = 3·9 c.p.s.

Uncoupled wing pitch frequency = 13·9 c.p.s.

TABLE 2

Variable Aspect Ratio—Constant Sweepback Wings

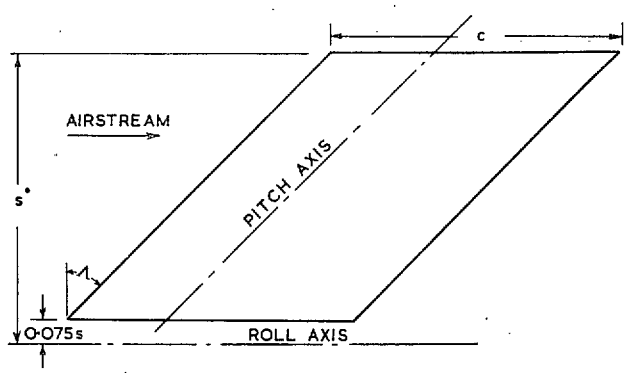

Wing chord, parallel to airstream, $c = 0{\cdot}5$ ft

$\frac{\text{Wing thickness}}{\text{Wing chord}}$ parallel to air-stream $= 0{\cdot}15$

Wing section $=$ RAE 101

$\frac{\text{Distance of pitch axis aft of leading edge}}{\text{Wing chord}} = 0{\cdot}35$

Wing sweepback A $= 45$ deg

Wing length root to tip s (in.)	Wing aspect ratio $(A = 2s/c)$	Inertias—wing plus mounting (slugs ft^2)		
		Roll inertia	Roll—pitch cross inertia	Pitch inertia
6	2·00	$1{\cdot}10 \times 10^{-3}$	$0{\cdot}94 \times 10^{-4}$	$7{\cdot}6 \times 10^{-5}$
7	2·33	$1{\cdot}78 \times 10^{-3}$	$1{\cdot}42 \times 10^{-4}$	$9{\cdot}1 \times 10^{-5}$
8	2·67	$2{\cdot}63 \times 10^{-3}$	$1{\cdot}82 \times 10^{-4}$	$10{\cdot}2 \times 10^{-5}$
9	3·00	$3{\cdot}76 \times 10^{-3}$	$2{\cdot}37 \times 10^{-4}$	$11{\cdot}8 \times 10^{-5}$
10	3·33	$5{\cdot}11 \times 10^{-3}$	$2{\cdot}67 \times 10^{-4}$	$13{\cdot}0 \times 10^{-5}$
12	4·00	$8{\cdot}82 \times 10^{-3}$	$3{\cdot}87 \times 10^{-4}$	$15{\cdot}4 \times 10^{-5}$
15	5·00	$17{\cdot}75 \times 10^{-3}$	$6{\cdot}45 \times 10^{-4}$	$20{\cdot}5 \times 10^{-5}$
18	6·00	$30{\cdot}27 \times 10^{-3}$	$8{\cdot}16 \times 10^{-4}$	$22{\cdot}9 \times 10^{-5}$

Uncoupled wing roll frequency $= 4{\cdot}0$ c.p.s.

Uncoupled wing pitch frequency $= 11{\cdot}0$ c.p.s.

TABLE 3

Constant Aspect Ratio—Variable Sweepback Wings

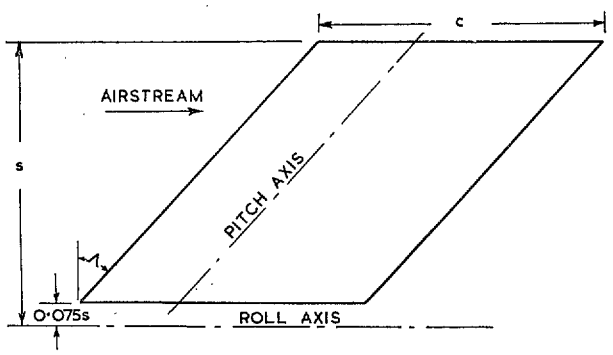

Wing chord parallel to air-stream, c = 0·5 ft

Wing length, root to tip, s = 0·667 ft

Wing aspect ratio $2s/c$ = 2·67

$\frac{\text{Wing thickness}}{\text{Wing chord}}$ parallel to airstream = 0·10

Wing section = RAE 101

$\frac{\text{Distance of pitch axis aft of leading edge}}{\text{Wing chord}}$ = 0·35

Wing Sweepback Λ (deg)	Inertias—wing plus mounting (slugs ft²)		
	Roll inertia	Roll—pitch cross inertia	Pitch inertia
0	$3{\cdot}52 \times 10^{-3}$	$1{\cdot}57 \times 10^{-4}$	$11{\cdot}02 \times 10^{-5}$
10	$3{\cdot}58 \times 10^{-3}$	$1{\cdot}64 \times 10^{-4}$	$10{\cdot}65 \times 10^{-5}$
20	$3{\cdot}62 \times 10^{-3}$	$1{\cdot}39 \times 10^{-4}$	$9{\cdot}24 \times 10^{-5}$
30	$3{\cdot}58 \times 10^{-3}$	$1{\cdot}44 \times 10^{-4}$	$8{\cdot}55 \times 10^{-5}$
45	$3{\cdot}64 \times 10^{-3}$	$1{\cdot}05 \times 10^{-4}$	$5{\cdot}50 \times 10^{-5}$
60	$3{\cdot}56 \times 10^{-3}$	$0{\cdot}74 \times 10^{-4}$	$2{\cdot}90 \times 10^{-5}$

Uncoupled wing roll frequency = 3·8 c.p.s.

Uncoupled wing pitch frequency = 11·2 c.p.s.

TABLE 4

Variable Aspect Ratio—Variable Sweepback Wings

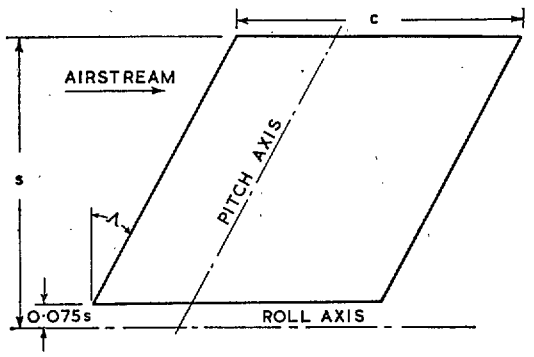

Wing chord, parallel to air-stream, $c = 0{\cdot}5 \sec \Lambda$ ft

Wing length root to tip, $s = 0{\cdot}667$ ft

$\frac{\text{Wing thickness}}{\text{Wing chord}}$ parallel to air-stream $= 0{\cdot}10 \cos \Lambda$

Wing section = RAE 101

$\frac{\text{Distance of pitch axis aft of leading edge}}{\text{Wing chord}} = 0{\cdot}35$

Wing chord c (ft)	Wing aspect ratio $(2s/c)$	Wing sweepback Λ (deg)	Inertias—wing plus mounting (slugs ft²)		
			Roll inertia	Roll—pitch cross inertia	Pitch inertia
0·500	2·67	0	$3{\cdot}57 \times 10^{-3}$	$1{\cdot}56 \times 10^{-4}$	$11{\cdot}3 \times 10^{-5}$
0·508	2·62	10	$3{\cdot}73 \times 10^{-3}$	$1{\cdot}60 \times 10^{-4}$	$11{\cdot}4 \times 10^{-5}$
0·577	2·31	30	$4{\cdot}20 \times 10^{-3}$	$1{\cdot}62 \times 10^{-4}$	$12{\cdot}5 \times 10^{-5}$
0·653	2·04	40	$4{\cdot}81 \times 10^{-3}$	$1{\cdot}83 \times 10^{-4}$	$14{\cdot}0 \times 10^{-5}$
0·778	1·72	50	$5{\cdot}73 \times 10^{-3}$	$2{\cdot}40 \times 10^{-4}$	$18{\cdot}9 \times 10^{-5}$

Uncoupled wing roll frequency = 3·5 c.p.s.

Uncoupled wing pitch frequency = 9·7 c.p.s.

TABLE 5

Variable Aspect Ratio—Tapered Wings

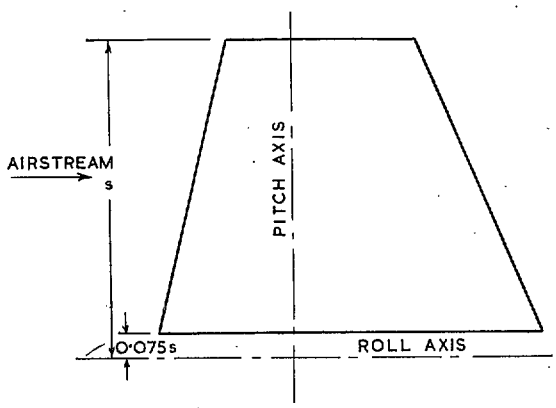

$\frac{\text{Wing tip chord}}{\text{Wing root chord}}$ = 0·5

Wing mean chord, c_m = 0·5 ft

Maximum thickness of wing section (constant along span) = 0·05 ft

Wing section = RAE 101

$\frac{\text{Distance of pitch axis aft of leading edge}}{\text{Wing chord}}$ = 0·35

Wing length root to tip s (in.)	Wing aspect ratio ($A = 2s/c_m$)	Leading edge sweep Λ (deg)	Trailing edge sweep Λ (deg)	Inertias—wing plus mounting (slugs ft²)		
				Roll inertia	Roll—pitch cross inertia	Pitch inertia
6	2·00	14·2	−25·1	$1·08 \times 10^{-3}$	$0·60 \times 10^{-4}$	$9·8 \times 10^{-5}$
7	2·33	12·2	−21·9	$1·74 \times 10^{-3}$	$1·07 \times 10^{-4}$	$12·7 \times 10^{-5}$
8	2·67	10·2	−19·3	$2·65 \times 10^{-3}$	$1·32 \times 10^{-4}$	$14·4 \times 10^{-5}$
9	3·00	9·5	−17·4	$3·76 \times 10^{-3}$	$1·69 \times 10^{-4}$	$15·8 \times 10^{-5}$
10	3·33	8·6	−15·7	$5·16 \times 10^{-3}$	$1·92 \times 10^{-4}$	$16·8 \times 10^{-5}$
12	4·00	7·2	−13·2	$9·20 \times 10^{-3}$	$2·96 \times 10^{-4}$	$20·7 \times 10^{-5}$
15	5·00	5·8	−10·6	$17·80 \times 10^{-3}$	$4·07 \times 10^{-4}$	$26·9 \times 10^{-5}$
18	6·00	4·8	− 8·9	$30·20 \times 10^{-3}$	$6·90 \times 10^{-4}$	$30·7 \times 10^{-5}$

Uncoupled wing roll frequency = 4·1 c.p.s.

Uncoupled wing pitch frequency = 13·2 c.p.s.

TABLE 6

Variable Aspect Ratio—Inverse Tapered Wings

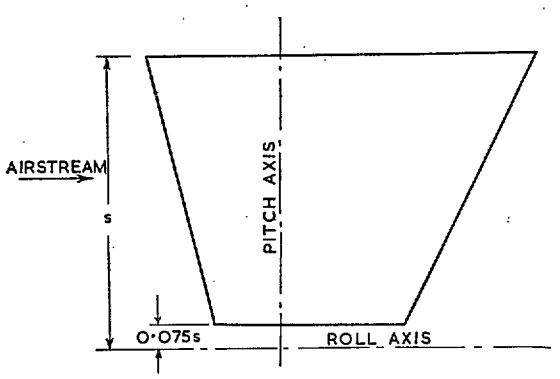

$\frac{\text{Wing tip chord}}{\text{Wing root chord}}$	$= 2{\cdot}0$
Wing mean chord, c_m	$= 0{\cdot}5$ ft
Maximum thickness of wing section (constant along the span)	$= 0{\cdot}05$ ft
Wing section	= RAE 101
$\frac{\text{Distance of pitch axis aft of leading edge}}{\text{Wing chord}}$	$= 0{\cdot}35$

Wing length root to tip s (in.)	Wing aspect ratio ($A = 2s/c_m$)	Leading edge sweep Λ (deg)	Trailing edge sweep Λ (deg)	Inertias—wing plus mounting (slugs ft^2)		
				Roll inertia	Roll—pitch cross inertia	Pitch inertia
6	2·00	−14·2	25·1	$1{\cdot}24 \times 10^{-3}$	$0{\cdot}88 \times 10^{-4}$	$9{\cdot}8 \times 10^{-5}$
7	2·33	−12·2	21·9	$2{\cdot}03 \times 10^{-3}$	$1{\cdot}55 \times 10^{-4}$	$12{\cdot}7 \times 10^{-5}$
8	2·67	−10·2	19·3	$3{\cdot}05 \times 10^{-3}$	$1{\cdot}92 \times 10^{-4}$	$14{\cdot}4 \times 10^{-5}$
9	3·00	− 9·5	17·4	$4{\cdot}31 \times 10^{-3}$	$2{\cdot}45 \times 10^{-4}$	$15{\cdot}8 \times 10^{-5}$
10	3·33	− 8·6	15·7	$5{\cdot}91 \times 10^{-3}$	$2{\cdot}79 \times 10^{-4}$	$16{\cdot}8 \times 10^{-5}$
12	4·00	− 7·2	13·2	$10{\cdot}60 \times 10^{-3}$	$4{\cdot}31 \times 10^{-4}$	$20{\cdot}7 \times 10^{-5}$
15	5·00	− 5·8	10·6	$20{\cdot}50 \times 10^{-3}$	$5{\cdot}91 \times 10^{-4}$	$26{\cdot}9 \times 10^{-5}$
18	6·00	− 4·8	8·9	$34{\cdot}70 \times 10^{-3}$	$10{\cdot}02 \times 10^{-4}$	$30{\cdot}7 \times 10^{-5}$

Uncoupled wing roll frequency = 3·8 c.p.s.

Uncoupled wing pitch frequency = 13·3 c.p.s.

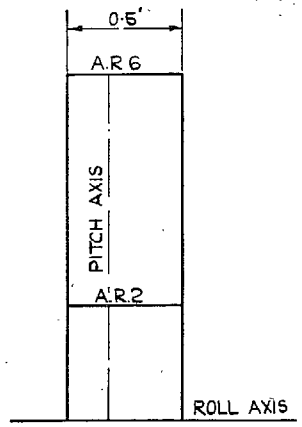

1a VARIABLE ASPECT RATIO, UNSWEPT WINGS.

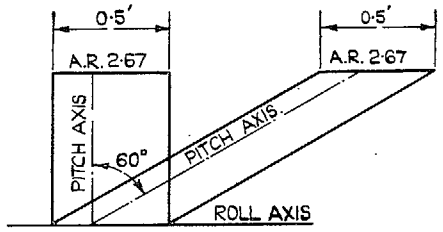

1c CONSTANT ASPECT RATIO, VARIABLE SWEEP WINGS.

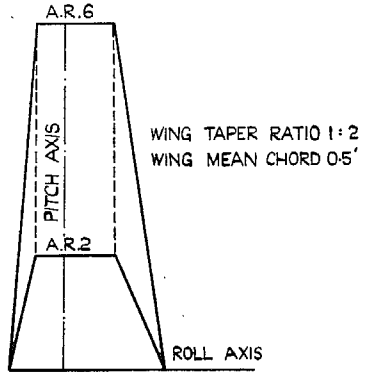

1e VARIABLE ASPECT RATIO, TAPERED WINGS.

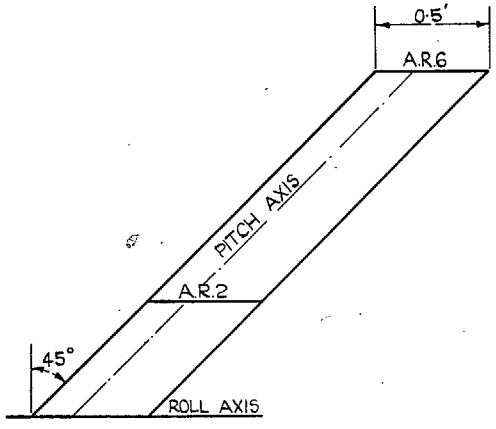

1b VARIABLE ASPECT RATIO, CONSTANT SWEEPBACK WINGS.

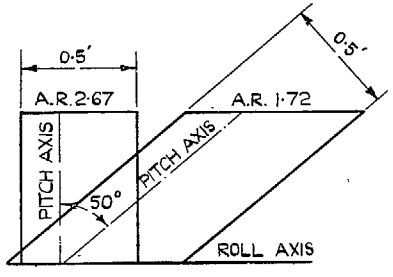

1d VARIABLE ASPECT RATIO, VARIABLE SWEEP WINGS.

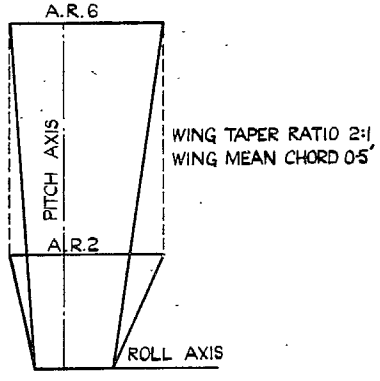

1f VARIABLE ASPECT RATIO, INVERSE TAPERED WINGS.

FIGS. 1a to 1f. Geometry of the wings.

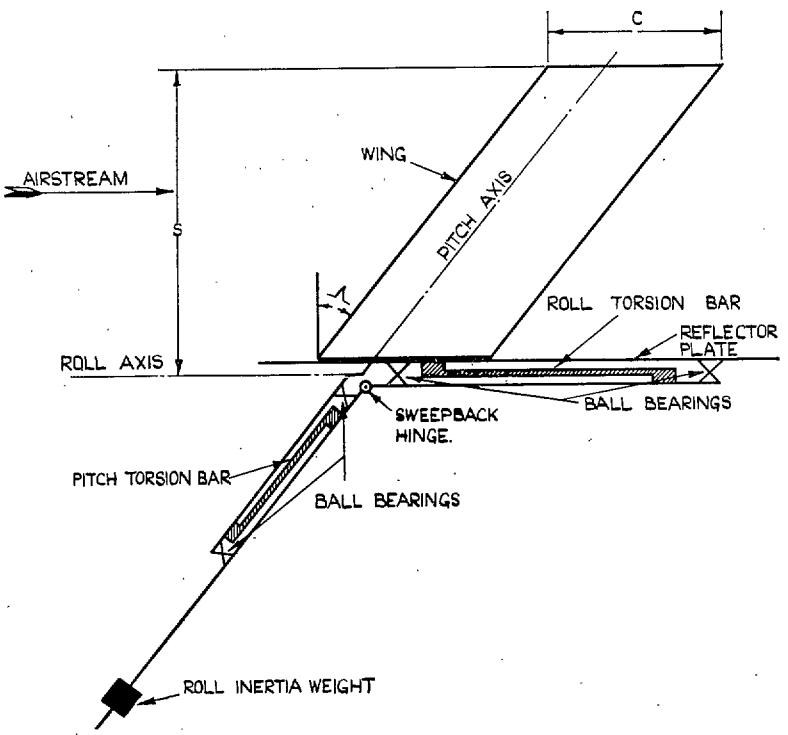

FIG. 2. Diagrammatic lay-out of flutter test rig.

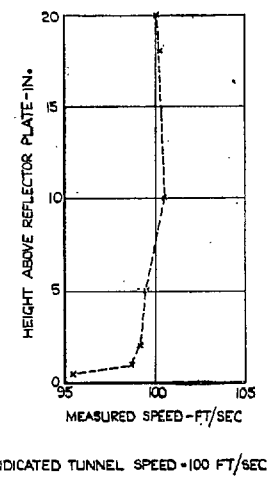

FIG. 3. Velocity distribution at wing position (R.A.E. 5-ft-Diameter Open Jet Wind Tunnel).

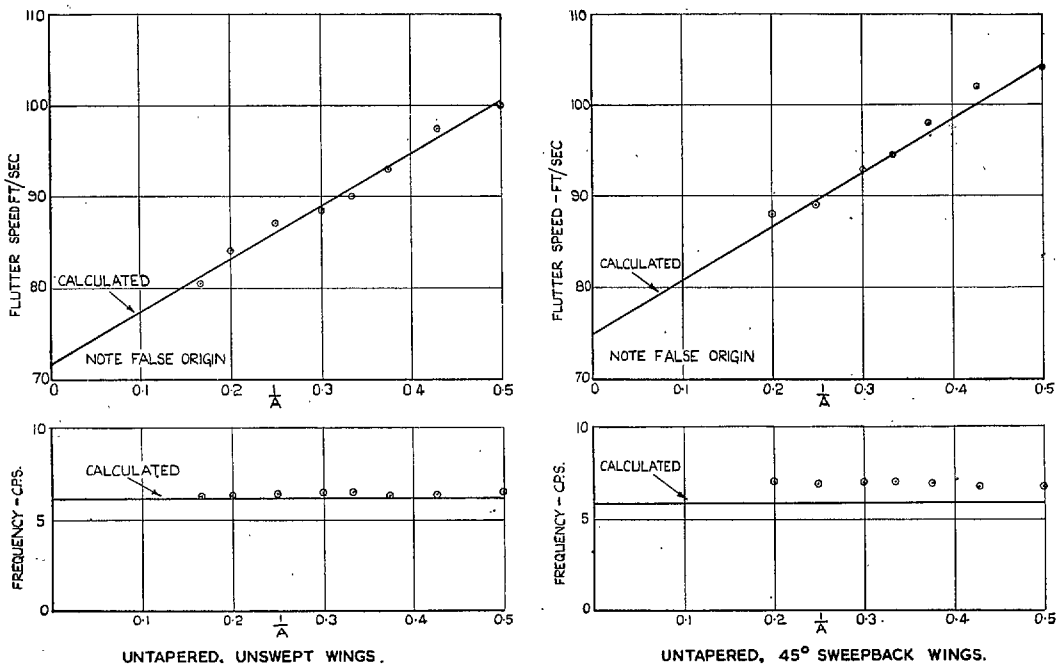

FIG. 4. The effect of aspect ratio on flutter speed and frequency for unswept and 45-deg swept wings.

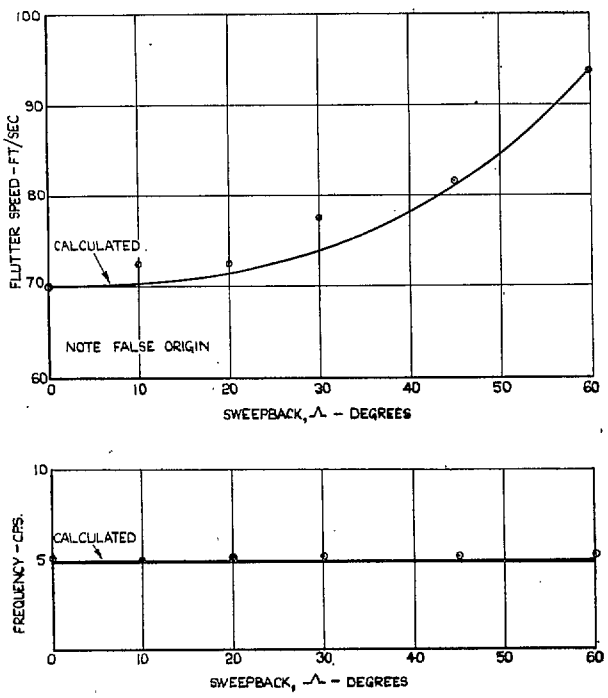

FIG. 5. The effect of sweepback on flutter speed and frequency for untapered wings of constant aspect ratio.

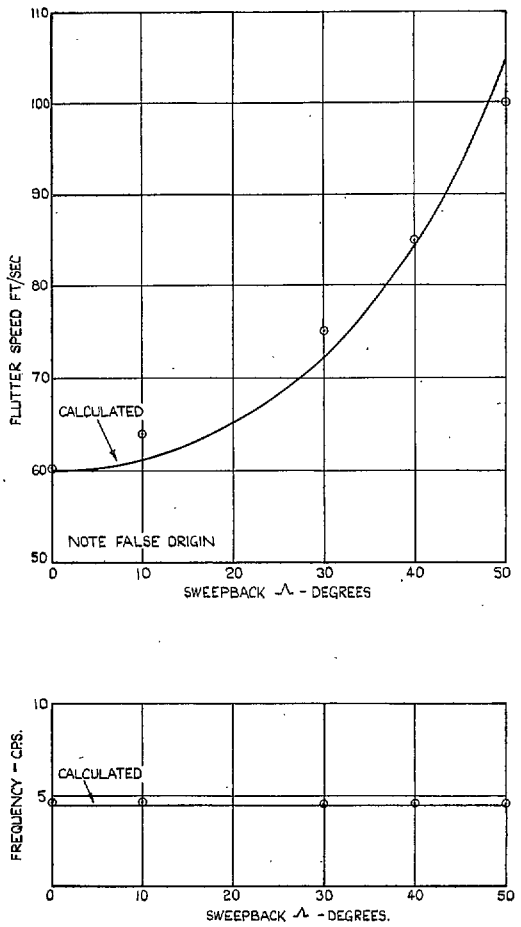

FIG. 6. The effect of sweepback on flutter speed and frequency for untapered wings of variable aspect ratio.

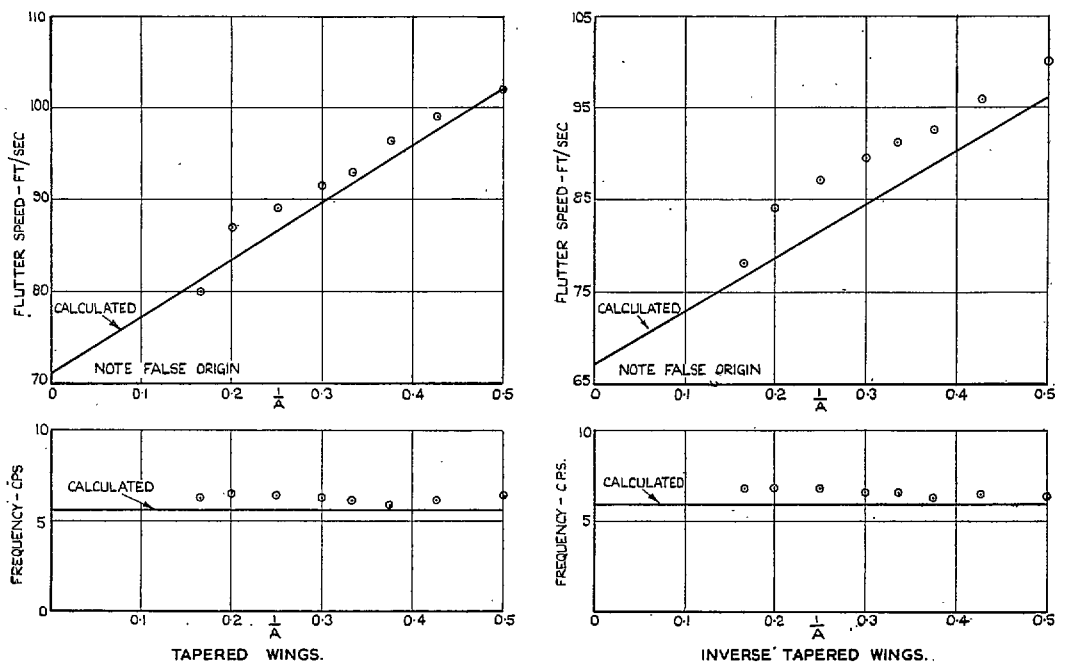

FIG. 7. The effect of aspect ratio on flutter speed and frequency for tapered and inverse tapered wings.

(5063) Wt. 20/9036 K.7 10/57 Hw. PRINTED IN GREAT BRITAIN

Publications of the Aeronautical Research Council

ANNUAL TECHNICAL REPORTS OF THE AERONAUTICAL RESEARCH COUNCIL (BOUND VOLUMES)

1939 Vol. I. Aerodynamics General, Performance, Airscrews, Engines. 50*s.* (51*s.* 9*d.*).
Vol. II. Stability and Control, Flutter and Vibration, Instruments, Structures, Seaplanes, etc. 63*s.* (64*s.* 9*d.*)

1940 Aero and Hydrodynamics, Aerofoils, Airscrews, Engines, Flutter, Icing, Stability and Control Structures, and a miscellaneous section. 50*s.* (51*s.* 9*d.*)

1941 Aero and Hydrodynamics, Aerofoils, Airscrews, Engines, Flutter, Stability and Control Structures. 63*s.* (64*s.* 9*d.*)

1942 Vol. I. Aero and Hydrodynamics, Aerofoils, Airscrews, Engines. 75*s.* (76*s.* 9*d.*)
Vol. II. Noise, Parachutes, Stability and Control, Structures, Vibration, Wind Tunnels. 47*s.* 6*d.* (49*s.* 3*d.*)

1943 Vol. I. Aerodynamics, Aerofoils, Airscrews. 80*s.* (81*s.* 9*d.*)
Vol. II. Engines, Flutter, Materials, Parachutes, Performance, Stability and Control, Structures. 90*s.* (92*s.* 6*d.*)

1944 Vol. I. Aero and Hydrodynamics, Aerofoils, Aircraft, Airscrews, Controls. 84*s.* (86*s.* 3*d.*)
Vol. II. Flutter and Vibration, Materials, Miscellaneous, Navigation, Parachutes, Performance, Plates and Panels, Stability, Structures, Test Equipment, Wind Tunnels. 84*s.* (86*s.* 3*d.*)

1945 Vol. I. Aero and Hydrodynamics, Aerofoils. 130*s.* (132*s.* 6*d.*)
Vol. II. Aircraft, Airscrews, Controls. 130*s.* (132*s.* 6*d.*)
Vol. III. Flutter and Vibration, Instruments, Miscellaneous, Parachutes, Plates and Panels, Propulsion. 130*s.* (132*s.* 3*d.*)
Vol. IV. Stability, Structures, Wind Tunnels, Wind Tunnel Technique. 130*s.* (132*s.* 3*d.*)

Annual Reports of the Aeronautical Research Council—
1937 2*s.* (2*s.* 2*d.*) 1938 1*s.* 6*d.* (1*s.* 8*d.*) 1939–48 3*s.* (3*s.* 3*d.*)

Index to all Reports and Memoranda published in the Annual Technical Reports, and separately—
April, 1950 - - - - R. & M. 2600 2*s.* 6*d.* (2*s.* 8*d.*)

Author Index to all Reports and Memoranda of the Aeronautical Research Council—
1909—January, 1954 R. & M. No. 2570 15*s.* (15*s.* 6*d.*)

Indexes to the Technical Reports of the Aeronautical Research Council—

December 1, 1936—June 30, 1939	R. & M. No. 1850	1*s.* 3*d.* (1*s.* 5*d.*)
July 1, 1939—June 30, 1945	R. & M. No. 1950	1*s.* (1*s.* 2*d.*)
July 1, 1945—June 30, 1946	R. & M. No. 2050	1*s.* (1*s.* 2*d.*)
July 1, 1946—December 31, 1946	R. & M. No. 2150	1*s.* 3*d.* (1*s.* 5*d.*)
January 1, 1947—June 30, 1947	R. & M. No. 2250	1*s.* 3*d.* (1*s.* 5*d.*)

Published Reports and Memoranda of the Aeronautical Research Council—

Between Nos. 2251–2349	R. & M. No. 2350	1*s.* 9*d.* (1*s.* 11*d.*)
Between Nos. 2351–2449	R. & M. No. 2450	2*s.* (2*s.* 2*d.*)
Between Nos. 2451–2549	R. & M. No. 2550	2*s.* 6*d.* (2*s.* 8*d.*)
Between Nos. 2551–2649	R. & M. No. 2650	2*s.* 6*d.* (2*s.* 8*d.*)

Prices in brackets include postage

HER MAJESTY'S STATIONERY OFFICE

York House, Kingsway, London, W.C.2; 423 Oxford Street, London, W.1; 13a Castle Street, Edinburgh 2; 39 King Street, Manchester 2; 2 Edmund Street, Birmingham 3; 109 St. Mary Street, Cardiff; Tower Lane, Bristol, 1; 80 Chichester Street, Belfast, *or through any bookseller*.

S.O. Code No. 23-3011